PROC. INST. ACOUSTICS VOL 7 PT 3 1985

DIFFRACTION OF A PLANE ACOUSTIC WAVE BY A LAYERED ELASTIC SPHERE

D. E. Busson

C.E.R.D.S.M. Le Brusc, 83140 SIX FOURS LES PLAGES, FRANCE

INTRODUCTION

The scattering of a plane acoustic wave propagating in a liquid by an elastic sphere is one of the few diffraction problems that can be solved analytically [1]. The calculation of the acoustic field diffracted by a sphere formed of several solid or liquid elastic layers follows the same techniques. In this paper, we present numerical results on the diffraction pattern of a hollow aluminium sphere whose thickness varies between 1 and 20 % of its radius, and by a sphere formed of one liquid layer enclosed between two aluminium layers. These results include plots of the total acoustic pressure on the surface of the spheres as functions of frequency for ka between 0 and 100, plots of the positions of the resonances of the spheres in the (frequency-harmonic number) plane, and sketches of the deformations induced in the spherical layers by the incident plane wave at resonance frequencies. Theoretical results are then compared with experimental measurements obtained on an aluminium hollow sphere.

THEORY

Let us consider a plane acoustic wave propagating in a fluid, incident on a sphere formed of several solid or fluid elastic concentric layers. The acoustic field outside the sphere and in its fluid layers is fully determined by its velocity potential Φ. The reference frame can be chosen so that the problem is axially symetric about the vertical axis, and the acoustic potentials, stresses and displacements do not depend on the azimuthal angle. A general solution for Φ in spherical coordinates is then:

$$\Phi = \sum_{n=1}^{\infty} (a_n j_n(kr) + b_n y_n(kr)) P_n(\cos\theta) \qquad (1)$$

j_n and y_n being spherical Bessel functions, P_n Legendre polynomials k the wave number in the fluid and r and θ the spherical coordinates. Two potentials are needed to describe the acoustic fields in a solid layer of the sphere: Φ, the scalar potential of longitudinal waves, and Ψ, the vector potential of shear waves. Φ can be written as a linear combination of spherical harmonics of the same type as the expression in Eq. (1), k being the wave number of longitudinal waves in the solid. Because of the azimuthal symetry of the geometry, Ψ has only one non-zero component, Ψ_φ, which can be written as:

$$\Psi_\varphi = \sum_{n=1}^{\infty} (c_n j_n(k'r) + d_n y_n(k'r)) \frac{dP_n}{d\theta} \qquad (2)$$

k' being the wave number of shear waves in the material. The acoustic displacements and stresses are computed from Eqs. (1) and (2), and expressed as linear combinations of Legendre polynomials

or of their derivative with respect to θ . The boundary conditions at an interface between two different materials are then written: continuity of the force applied on any type of interface, continuity of the radial displacement at a fluid-fluid or fluid-solid interface and of the total displacement at a solid-solid interface. Finally, the incident plane wave potential is decomposed in a series of spherical harmonics.
Because of the orthogonality properties of the Legendre polynomials and of their derivatives with respect to θ , the calculation of the unknown constants appearing in Eqs. (1) and (2) is reduced to the resolution of one system of linear equations with complex coefficients for each spherical harmonic considered. Theoretically, an infinite number of spherical harmonics is needed to write the exact acoustic field inside and outside the sphere. In practice the convergence of the series is obtained with less than 2ka terms.

A FORTRAN routine has been written to calculate the acoustic field diffracted by an elastic layered sphere. From the geometry of the sphere, and from the acoustic characteristics of the materials used in the different layers, the program generates and solves the linear system of equations associated with each spherical harmonic. It will accept spheres formed of up to 9 solid or fluid layers. The frequency range that can be studied for a given sphere extends from 0 to a frequency such that ka is of the order of 100 (k being in this case the largest wave number used in the problem). The absorbing properties of lossy materials are modelled by the use of complex celerities.
Several types of results can be obtained from this program. The acoustic pressure scattered by the sphere or the total acoustic pressure around the sphere can be plotted as functions of the frequency of the incident wave or of the position of the observation point. Colour-coded maps of the modulus of the acoustic pressure around the sphere and in its fluid layers, and of the radial component of stress in its solid layers, and images of the deformations induced in the sphere's layers by the incident wave are also produced.

NUMERICAL RESULTS

To demonstrate its capabilities, we have calculated the acoustic field scattered by a hollow aluminium sphere, for several values of the b/a ratio of the inside radius of the sphere to its outside radius, and by a hollow sphere formed of three concentric layers, one water layer separating two aluminium layers. The outside radius of all spheres is 0.239 m, so that the value of the product ka of the wave number in the exterior fluid (water) by the outside radius of the sphere is equal to the frequency of the incident wave in kHz. The following parameters are used:
for water ρ=1030 kg/m3, C=1500 m/s
for aluminium ρ=2700 kg/m3, Cl=6300 m/s, Cs=3100 m/s.
The fluid filling the spheres is supposed to be perfectly soft.
Hollow spheres.
Figures 1 to 5 show the evolution of the characteristics of the acoustic field scattered by a hollow aluminium sphere when the b/a ratio is reduced from 0.99 to 0.8. Each figure is formed of two parts. The top plot is a plot of the total acoustic pressure in front of the sphere on its outer surface, normalised by the

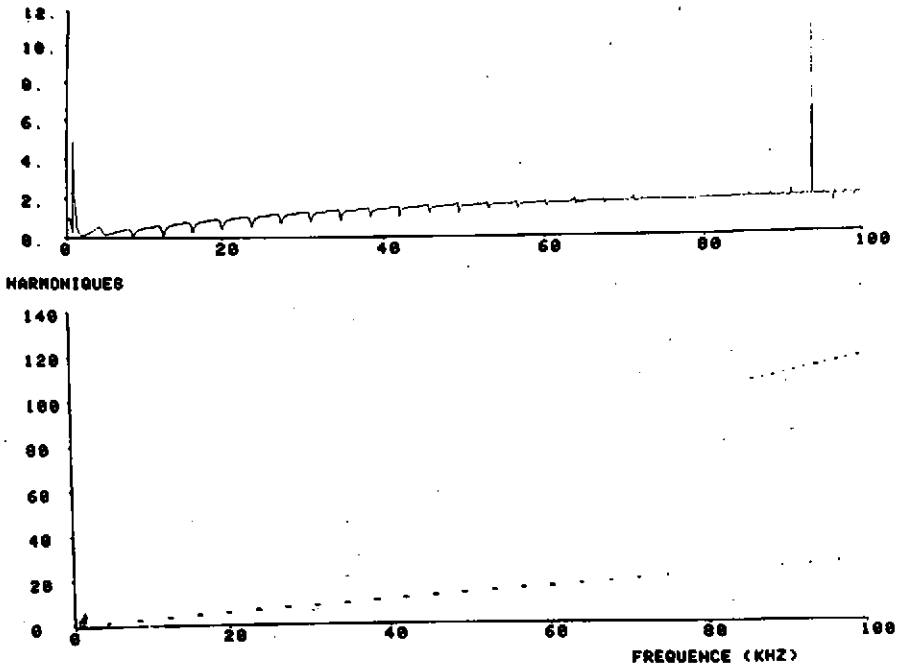

Figure 1: Hollow aluminium sphere, b/a=0.99

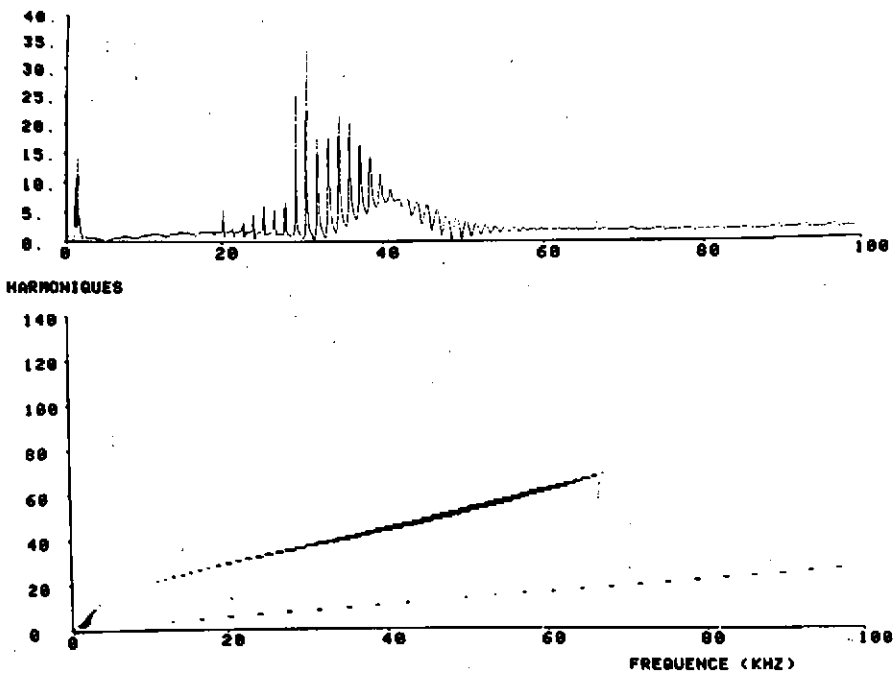

Figure 2: Hollow aluminium sphere, b/a=0.97

value of the pressure of the incident wave, as a function of frequency for ka between 0 and 100. From figure 1, for example, it is clear that the total pressure on the sphere is the sum of two parts: a background which varies smoothly with frequency, and several series of resonances which appear on the plot as sharp peaks. This function of frequency is also the sum of a series, each term being the product of a spherical Hankel function (which describes the outgoing diffracted wave) by a complex coefficient. Whereas several coefficients contribute to form the smooth background at a given frequency, a resonance peak of the acoustic pressure is present in only one spherical harmonic coefficient. A resonance appears when the perimeter of the sphere is equal to n+1/2 wavelengths of a guided wave, excited in the shell by the incident plane wave. It is then possible to group the resonances of the sphere in several families associated with the different types of guided waves that can propagate in a plate or a shell. This is usually done by searching, for each spherical harmonic n, the complex values of the frequency that null the denominator of the nth coefficient [2]. But searching the roots of a complicated function in the complex plane is not simple. The method presented here allows for the determination of the order of a given resonance, and the separation of the resonances of the sphere in families, using very simple signal processing techniques. Each coefficient of the decomposition of the diffracted acoustic field in spherical harmonics is considered as a signal, function of frequency. To isolate the resonances form the rest of the curve, an average background is substracted from the total coefficient. This is easily done by filtering the signal with a high-pass filter. The resonances are then detected by comparing the filtered signal to a given threshold. But our signal is a function of frequency, and filtering a function of frequency with a high-pass filter corresponds, in the time domain, to suppressing the specular echoes reflected by the sphere, and keeping only the echoes arriving after the specular reflection, those having travelled through the sphere or around its surface. In the bottom part of each figure are plotted, in the (frequency-harmonic number) plane, the filtered coefficients of the decomposition in spherical harmonics of the potential diffracted by the spheres. The black dots correspond to points where the filtered coefficient is larger than the threshold.

The results plotted in figure 1 were obtained with b/a=0.99. The resonances of the sphere can be separated in three families. The first series (noted A) appears at very low frequencies only, and is characterised in the total pressure plot by very sharp peaks. The second series (noted B) is present in the whole frequency range. It generates broad dips in the top plot, regularly spaced along the frequency axis. The third series which will be noted A' appears only at very high frequencies, above 80 kHz. When the thickness of the shell is increased to b/a=0.97 (figure 2), the resonances of the B series are almost unperturbed. But the resonances of the A' series appear now at much lower frequencies, between ka=20 and ka=65. If b/a is increased to 0.95, the A and A' series merge into a single mode of resonance. This shows that in fact the resonances of the A and A' series in figures 1, 2 and 3 are due to the same type of wave propagating around the sphere. The resonances of this mode which are missing in figure 1

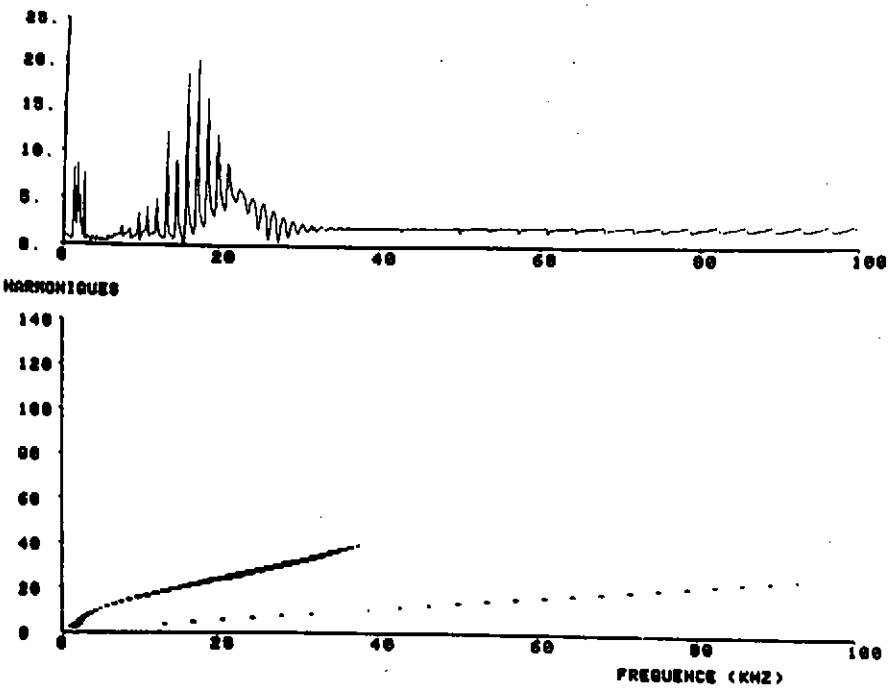

Figure 3: Hollow aluminium sphere, b/a=0.95

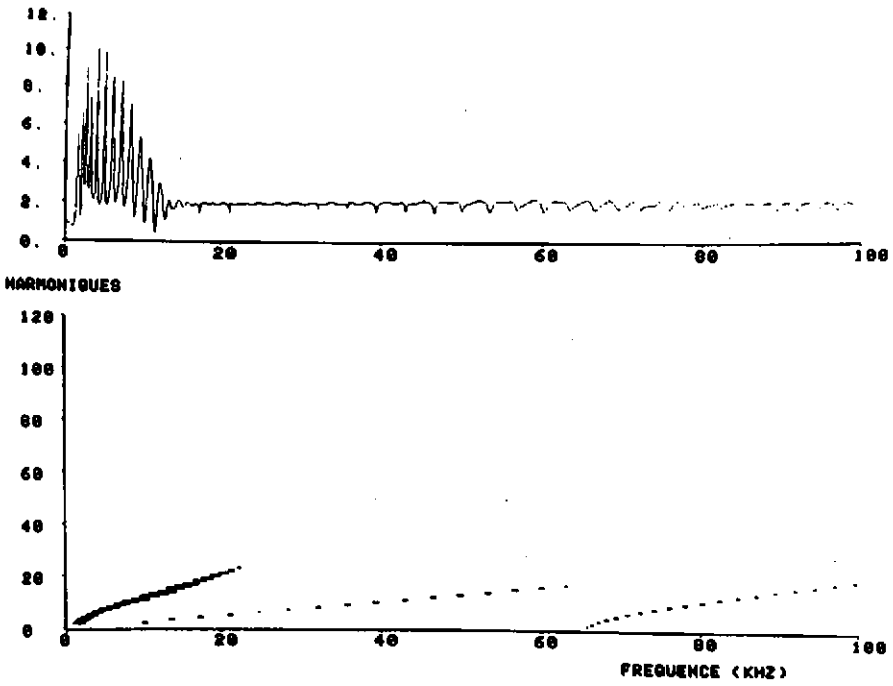

Figure 4: Hollow aluminium sphere, b/a=0.90

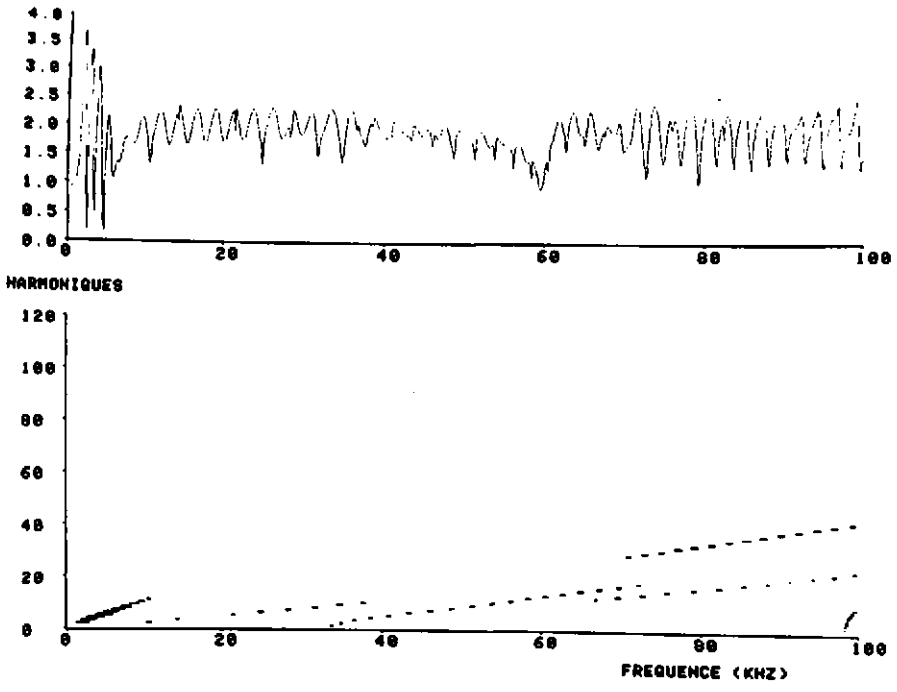

Figure 5: Hollow aluminium sphere, b/a=0.80

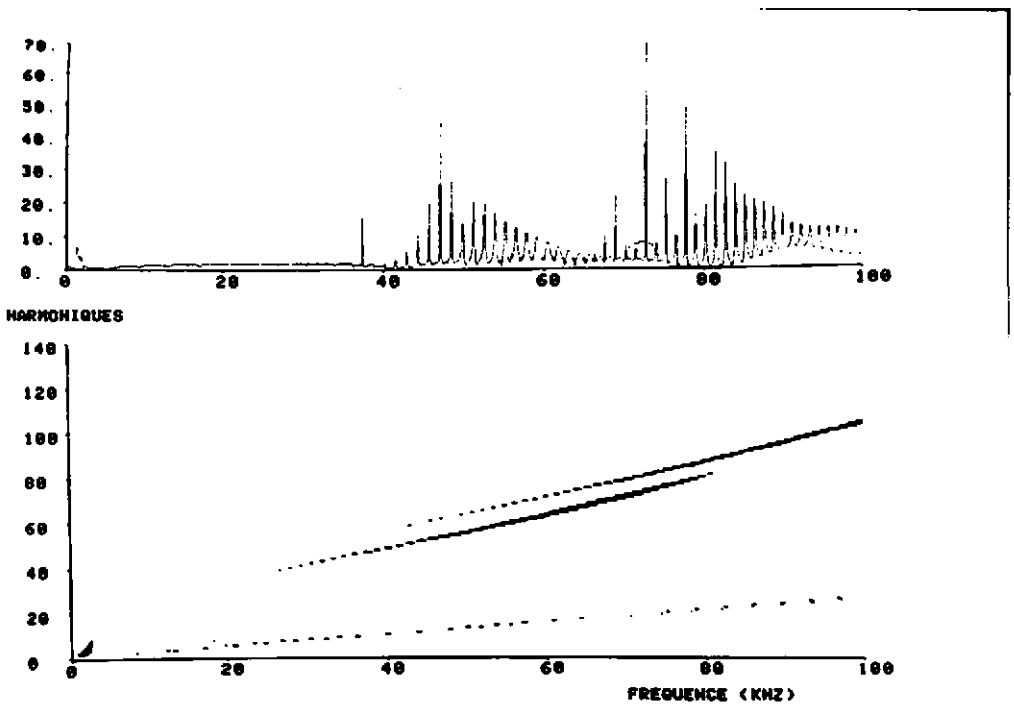

Figure 6: Sphere formed of three layers

(between ka=2 and ka=80) and in figure 2 (between ka=5 and ka=10) exist probably, but are too weak to be detected. At b/a=0.90 (figure 4) a third mode of resonance appears around ka=65. At b/a=0.80 (figure 5), the starting point of this mode on the frequency axis is around ka=33, and three other modes appear in the high frequency part of the plot. The analogy between the four first plots and the dispersion curves of Lamb wave modes in a plate is striking. Resonances of type A are probably due to the excitation of the first antisymetric Lamb wave mode in the shell; the very high dispersion of this mode a low frequencies explain the curved shape of the line formed by the resonances in the (frequency-harmonic number) plane in figures 2 and 3. Resonances of type B would then be those of the first symetric Lamb wave mode. This mode is not dispersive at low frequencies, and this explains why the positions of its resonances are almost unchanged when b/a is decreased. The third mode appearing in figure 4 is probably the second antisymetric Lamb wave mode.

We have drawn in figures 7, 8 and 9 the (exagerated) computed deformations induced in the sphere with b/a=0.99 at a given instant in time, at three frequencies corresponding to the first three resonance peaks of the A series. At the first resonance frequency, for ka=0.76 (figure 7), the sphere is deformed in an ellipsoidal shape, characteristic of a mode of order 2. In figure 8, for ka=0.96, the sphere is deformed in a pear shaped shell: this is a resonance of order 3. For ka=1.12, corresponding to a resonance of order 4, the cross section of the sphere takes a square shape. The antisymetry of the acoustic displacements about the middle line of the shell confirms that the resonances of the A series are due to the first antisymetric Lamb wave mode.

Sphere formed of three layers

This sphere is formed of three layers of equal thickness 0.48 cm (2% of the sphere's radius), one water layer between two aluminium layers. Figure 6 shows the total acoustic pressure in front of the sphere for ka between 0 and 100, and the position of its resonances in the (frequency-harmonic number) plane. Two different series of resonances of type A appear at high frequencies at positions which seem characteristic of a shell of b/a ratio close to 0.98. These are the resonances of the two aluminium shells, vibrating independantly of each other. The B series of resonances is also doubled. Figure 10 shows the deformations of the three layers for ka=4.28, corresponding to the resonance of order 1 of the B series.

EXPERIMENTAL RESULTS

In order to test the validity of our model, we have performed experimental measurements of the acoustic pressure field around a hollow aluminium sphere of outside diameter 20 cm, of thickness 1 cm (b/a=0.90), insonified by a plane wave. This sphere had been built for other purposes, and was not perfect. It was formed of two half spheres screwed together. Twelve cylindrical 1 cm diameter holes drilled through the shell had been filled with aluminium plugs. The receiver, placed in the sphere's equatorial plane, 10 cm away from the sphere's surface, recorded the total acoustic pressure,sum of the pressures of the incident plane wave and of the diffracted wave, as a function of the angle of rotation of the sphere, at several frequencies between 10 and 100 kHz.

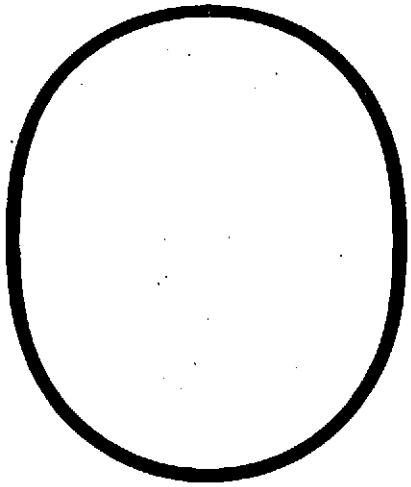

Fig. 7: b/a=0.99, ka=0.76

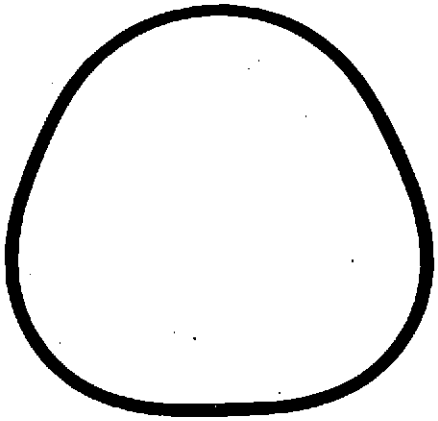

Fig 8: b/a=0.99, ka=0.96

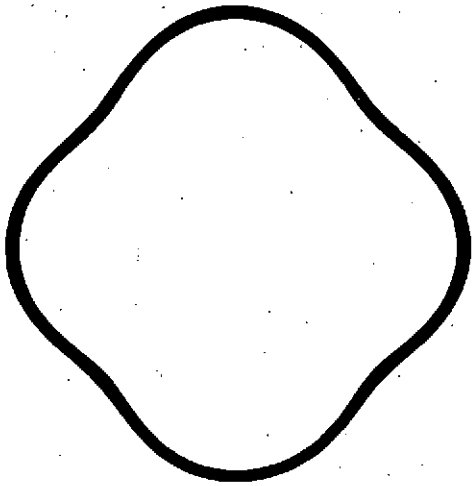

Fig 9: b/a=0.99, ka=1.12

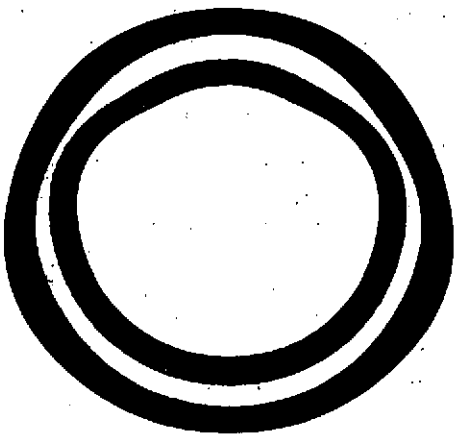

Fig 10: Three layers, ka=4.28

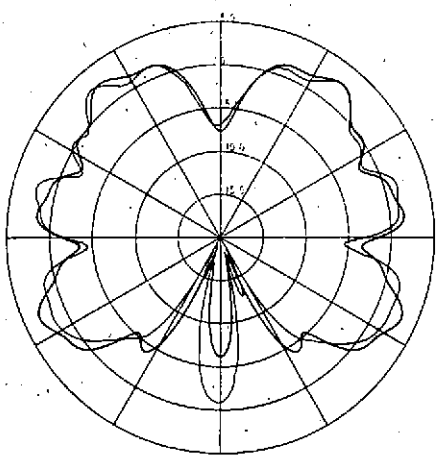

Figure 11: Frequency 19 kHz

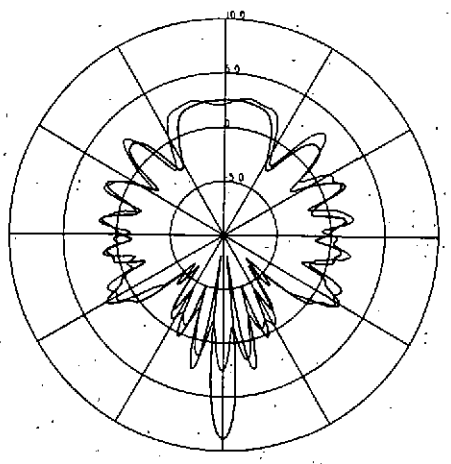

Fig 12: Frequency 38 kHz

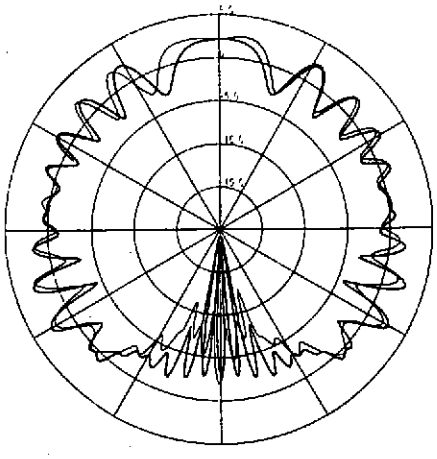

Fig 13: Frequency 66 kHz

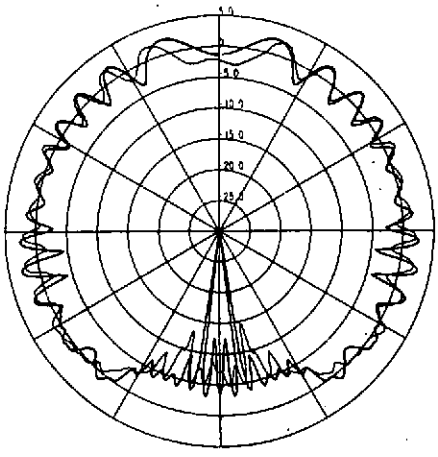

Fig 14: Frequency 83.86 kHz

Figures 11 to 14 show the comparison between theoretical and experimental results at four frequencies, respectively 19, 38, 66 and 83.86 kHz. In each picture the plane wave is incident on the sphere from the top of the drawing. The heavier line is the plot of the total pressure calculated from our model, in decibels, and the lighter line the plot of the experimental results. The agreement between the two sets of results is excellent. The positions and amplitudes of the different lobes of the experimental patterns are very well predicted by the theory. Small differences appear principally on the back of the sphere, in the sidelobes of the pressure field. They are probably caused by the imperfections of the sphere, which tend to attenuate the guided waves propagating in the shell, and also to the finite size of the receiving transducer which averages the pressure field over the volume of its active element. For the same reasons we were unable to detect any of the resonances predicted by the theory in the frequency range of the experiment (ka from 4 to 40).

CONCLUSIONS

A computer program has been developed to calculate the acoustic field diffracted by an elastic layered sphere, insonified by a plane wave. It will solve the case of spheres formed by up to nine layers, for frequencies up to ka=100. A simple signal processing method is used to isolate the resonances of the elastic shells, to identify their order and group them into resonance modes corresponding probably to Lamb wave modes. Experimental results, obtained on an aluminium hollow sphere of b/a ratio 0.90 confirm the validity of our theoretical model.

REFERENCE

1 :J.J. FARAN "Sound scattering by solid cylinders and spheres", JASA 23 (4) p 405 (1951)
2 :H. UBERALL, L.R. DRAGONETTE, L. FLAX "Relation between creeping waves and normal modes of vibration of a curved body" JASA 61 (3) p 711 (1977)
3 :B. AULD "Acoustic fields and waves in solids" J. Wiley and Sons, New York 1973